Experimental investigation of a Single Droplet Interaction with Shear Driven Film

S. K. Alghoul*, C. N. Eastwick, and D. B. Hann
Division of Energy and Sustainability, Faculty of Engineering
University of Nottingham
Nottingham, NG7 2RD, UK

Abstract

The main objective of this work is to visualize and clarify the outcomes of a water droplet interaction with water shear-driven film in rectangular duct. Droplet diameters used in this study ranging from 2.4 to 4.8 mm. The shearing air velocity is between 4.5 and 15 m/s and the water film thickness is between 0.2 and 1.7 mm. Two high speed cameras are used to track the droplet and visualize the film surface. A laser focus displacement meter (LFDM) is used to obtain the instantaneous and average film thickness. By analyzing the acquired images along with the film thickness different regimes for both droplet deformations in shearing air and impact outcomes are observed. A regime map is produced relating the air, film and droplet properties with the outcomes of the interaction between the droplet and the moving water film.

Introduction

The impact of liquid droplets onto moving liquid films is of great interest in many industrial applications, for example cooling flows within the power generation industry, in cylinder flows within car engines and lubrications flows within aeroengines. Previous research has focused on the impact of droplets onto static films, for example[1]. Although published research [2, 3] has investigated droplets in shear-driven liquids, there was no published work that shows detailed aspects of the dynamics of the impact of single droplet with shear-driven film.

This paper is one of a series of papers by the authors investigating the impact of droplets onto moving liquid films [4].The case considered in this paper is the impact of a single water droplet upon a shear-driven water film in rectangular duct. Figure 1 shows a schematic of the problem where a single droplet is ejected vertically through the air to impact upon a wavy film. The impact occurs at a section of the duct where both the air and water film flows are fully developed. When the air velocity is high enough the air deforms the droplet and changes its path. At higher air velocities the droplet is expected to breakup due to the shearing air force before it impacts the film.

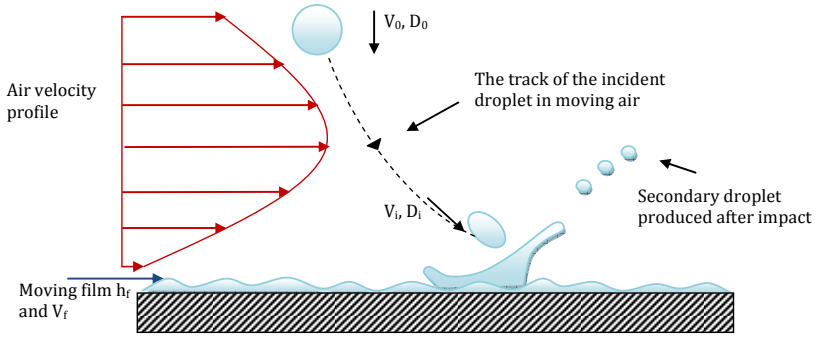

Figure 1. Schematic of the problem

The main aim of this study is to visualize and clarify the impact phenomena and its outcomes. The effect of different parameters on the impact outcomes is studied by establishing a regime maps for different droplet sizes. Images of the droplet deformation at different air velocities and also images of the impact outcomes are presented within the paper.

* Corresponding author: eaxsa1@nottingham.ac.uk

Experimental work

The shear-driven film rig used in this work is shown in Figure 2. The main part of the rig is the transparent rectangular duct (25x161x2000 mm) through which the air (4.5 – 15 m/s) is blown over a thin water film (0.2 – 1.7 mm). The duct has an inclination of one degree dropping from downstream to upstream. For more details about the design, instrumentation and other procedures regarding this rig see reference [5]. The test section is placed about one meter from the entrance where the air and the film are fully developed [5]. At the test section a droplet is generated by using a syringe pump which ejects a droplet through a sealed vertical tube mounted on the duct (see Figure 2). Droplet diameters used in this experiment range from 2.4 to 4.8 mm.

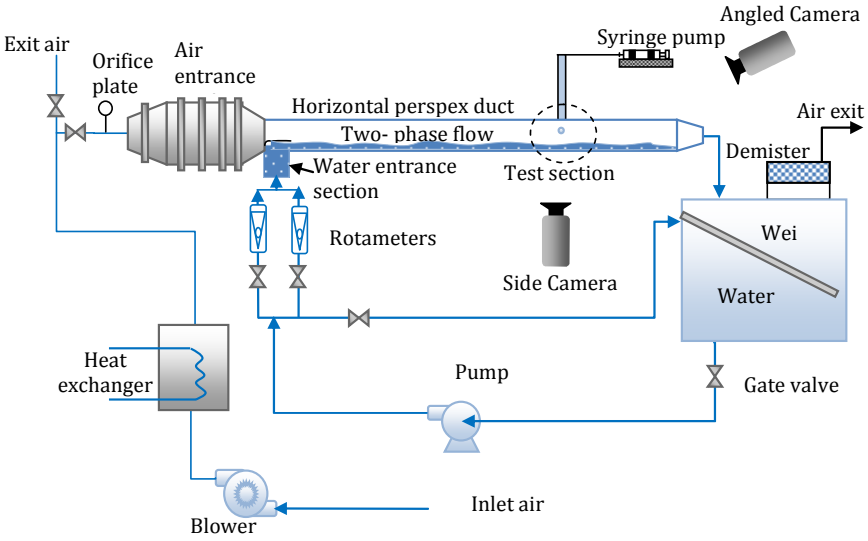

Figure 2. Schematic of the experimental rig

Operating conditions

The film width is 161 mm and is produced with liquid pumped into the duct and then driven by the shearing air. Table 1 summarizes the operating conditions for the experiment and the properties of water and air are shown in table 2 below. The measurements presented in this paper have been conducted using tap water

Table 1. Operating conditions of droplets and film

Droplet diameters (mm)	2.4, 2.8, 3.8, 4.8
Droplet Weber number	93-381
Duct/film width (mm)	161
Duct height (mm)	25
Duct length (m)	2
Impact point section (mm)	1060
Water flow rate per duct width/ film loading (cm^2/s)	0.36-2.28
Average air velocity (m/s)	4.5 -16.0
Ambient temperature (°C)	17 - 20

Table 2. Fluids properties

Property / Fluid	water	air
Viscosity (Ns/m^2) (from standard tables)	$1x10^{-3}$	$1.8x10^{-5}$
Density (kg/m^3) (measured)	998	1.22
Surface tension (J/m^2) (measured)	0.072	

Experimental procedure

General experimental procedures for the rig have been shown in [5]. The different elements of this experiment are the droplet generator which are similar to those described in [4]. After adjusting the rig setting of the air velocity and the water flow rate a droplet is produced using the syringe pump shown in Figure 2. The droplet falls through a sealed vertical tube before entering the rig and then falls through the shearing air ultimately impacting the shear-driven water film.

Two high-speed cameras were synchronized to track the droplet movement from the side and above the duct as shown in Figure 2. The side camera is aligned perpendicular to the duct side which allows a geometrical analysis for the falling droplet. The camera above is inclined about 46° to the horizontal so that the wave regimes of the water film can be investigated for identification of regime boundaries for the surface waves. Moreover, this camera allowed the observation of the droplet shape in another plane during the deformation in the shearing air which gives a better idea about the impact process. The high speed system setup including cameras, lights and the diffusers are similar to those described in [4].

The instantaneous and average film thickness are obtained with high accuracy by using a laser focus displacement meter (Keyence LT-9030) film thickness measurement device. A data acquisition card is used to take the voltage output from the LFDM device and transfer it to a computer where the data is calibrated and analyzed.

All devices used in this experiment were calibrated to ensure that the provided results are accurate. The repeatability of the rig is tested by measuring the average thickness of the shear driven film (using LFDM) at certain air /water flow rates settings and the results shown in Figure 3 suggest that the rig can provide very repeatable results.

Results and Discussion

After calibrating all the experimental data and processing the acquired images the results of this work are categorized mainly in four sections; Film thickness analysis, surface wave patterns, droplet deformation and breakup in shearing air and finally the impact outcomes.

Shear-driven Film Thickness

The average film thicknesses acquired by using Laser Focus Displacement Meter (LFDM, Keyence LT-9030) are shown in Figure 3. The error in measuring the average film thickness is very small as illustrated by the error bars and it decreases for thinner films due to the decrease of the amplitude of the surface waves.

The figure shows that increasing air velocity leads to a decrease in film thickness as a result of the increase in the shear stress at the interface between air and water. Increasing the water flow rate leads to increase in the film thickness for air velocities up to 13m/s due to the conservation of mass. At an air velocity of 14m/s the film thickness increases with water flow rate up to 1.2 cm^2/s after that the film thickness is nearly constant. Figure 4 illustrates this behaviour in dimensionless parameters where the film thickness stays constant by increasing the film Reynolds number above 123 for a range of Weber numbers between 140 and 225.

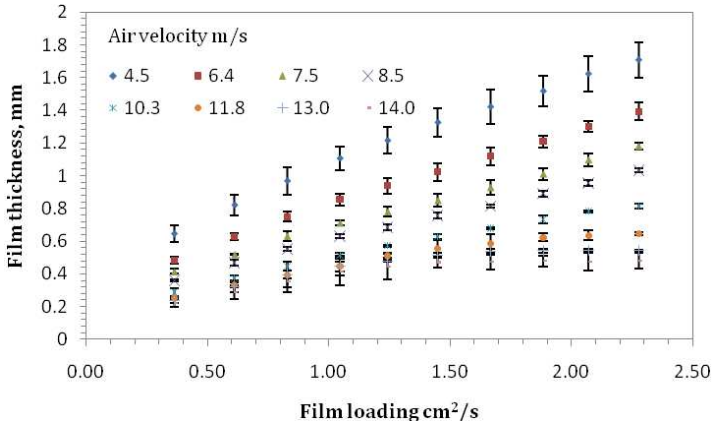

Figure 3. Measured film thickness for different water and air flow settings.

The maximum film thickness obtained is 1.75 mm with a minimum air velocity of 4.5 m/s and maximum water film loading of 2.28cm^2/s. While the minimum film thickness is 0.22mm, which occurred at the maximum air velocity of 14.0 m/s and the minimum film loading 0.36cm^2/s.

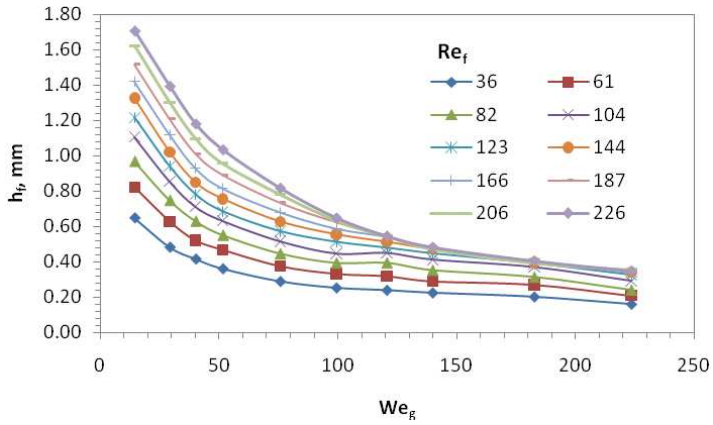

Figure 4. Measured film thickness for different film Reynolds numbers.

Surface Wave Patterns

Wave patterns which were observed by using the high speed camera above the duct are; 2 dimensional waves, 3 dimensional waves and roll waves. The transitions between theses regimes are shown as continues lines in Figure 5. The transitions between these regimes are not sharp and happen across some points where two different wave types exist, i.e., 2D and 3D waves or 3D and roll waves. Table 1 shows the exact conditions for some selected points. Most of the impact cases obtained in this experiment are onto 3D wave films, while a few cases are onto 2D and roll wave films.

Increasing film and/or air velocity leads to transition from 2D waves to 3D waves and then to roll waves. This transition leads to a decrease in the surface waves' amplitudes as shown in Figure 6. This figure also shows that the maximum amplitude of the surface waves is about 0.5 mm, which is about 5 times smaller than the smallest droplet used (2.4mm) in the current work. It is expected that due to the difference in the order of magnitude of the waves' amplitudes and the droplet diameter and also due the fact that the film velocity is low, the surface waves will not have an important influence on the impact outcomes.

Table 1. Two phase flow conditions for some selected points

	A	B	D
Average air velocity (m/s)	4.5	14.0	14.0
Film loading (cm^2/s)	0.36	0.36	2.28
Average film thickness (mm)	0.65	0.22	0.48
Surface wave regime	2D	3D	Roll

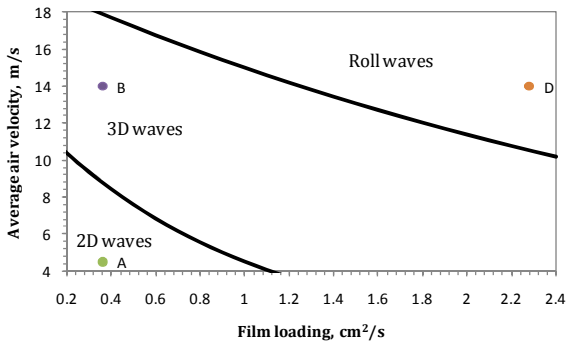

Figure 5. Transition boundaries for the patterns of the film surface waves

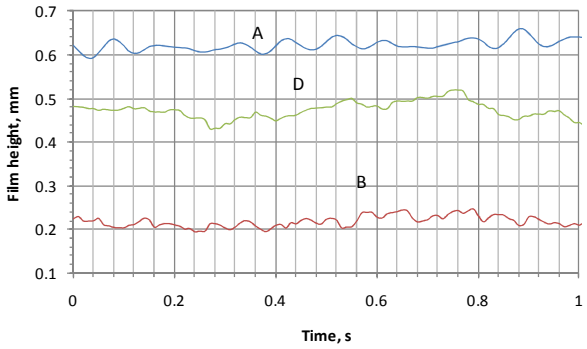

Figure 6. Instantaneous measurement of the film surface

Droplet deformation and breakup in shearing air

When a water droplet enters the duct, aerodynamic forces might cause it to deform and breakup. Figure 7 shows the images of a 2.4mm droplet falling in shearing air. Every image is reproduced by superimposing the corresponding sequence of images together using a Matlab program written especially for this purpose. The droplets enter the duct at a velocity of 2.4m/s.

At shearing air velocities of 4.5 – 6.4m/s (Figure 7i-ii) droplets fall vertically and a very slight deformation is observed when the droplet across the middle of the duct. At velocities of 8.5m/s up to 11.8 m/s (figure 7iii-v) the drag force on the droplet affects the droplet trajectory forcing it to the right and the droplet is clearly deformed in these cases. Increasing the air velocity to13.0 m/s deforms the droplet into a bag shape as shown in Figure 7-vi. An interesting phenomenon is observed for the range of air velocities up to 13.0m/s that the droplet recovers to a spherical shape just before it impacts the duct surface.

By increasing the air velocity to 14m/s the droplet deforms gradually and it takes the shape of a bag. The bag (droplet) eventually breaks up near the duct bottom through a bag break up mechanism [6-8]. This type of break up is referred to as a secondary atomization [8]. For higher shearing air velocities the break up occurs but is quicker than the previous case, i.e., it happens closer to the duct top.

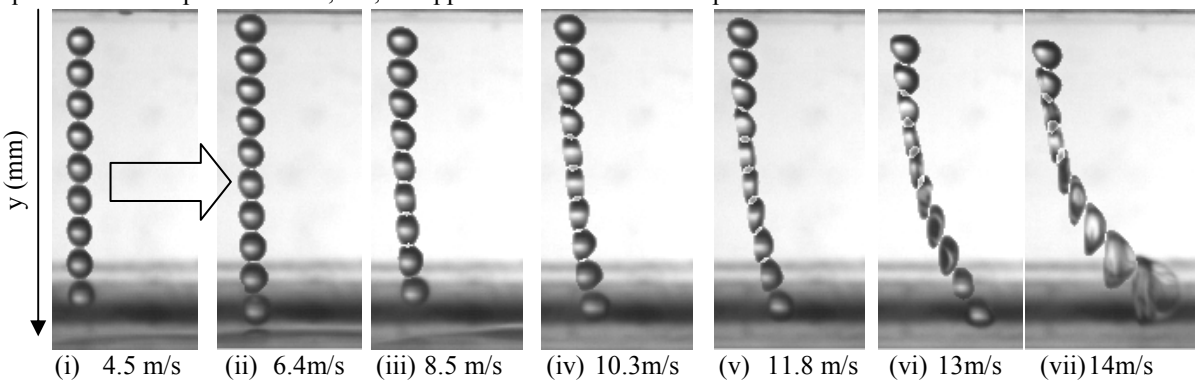

Figure 7. Deformation of 2.4 mm droplet in shearing air of different velocities, horizontal arrow shows the direction of the shearing air.

Figure 8 shows the velocity profiles for those droplets shown in Figure 7. The velocity of the droplet seems to be constant and equal to the droplet velocity at the entrance for cases i to vi. The small fluctuations in the velocity values shown in this figure are found to be within the experimental error. For the last case (Figure 7 vii) the droplet velocity increases noticeably up to approximately 3.1 m/s. The drag force on the droplet, due to shearing air, flattens the droplet and increases the drag area. Consequently the drag force increases and raises the horizontal component of the droplet velocity as shown Figure 9. The horizontal velocity component for the falling droplet increases as the shearing air velocity increases.

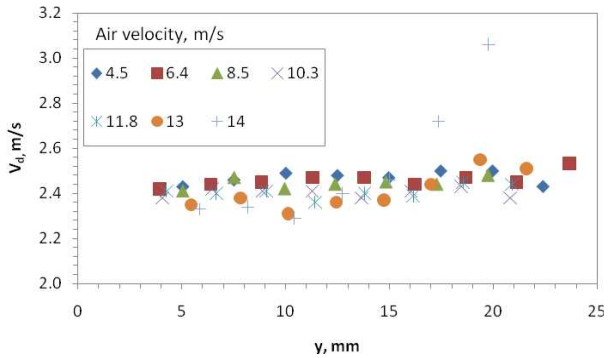

Figure 8. Droplets velocity in shearing air

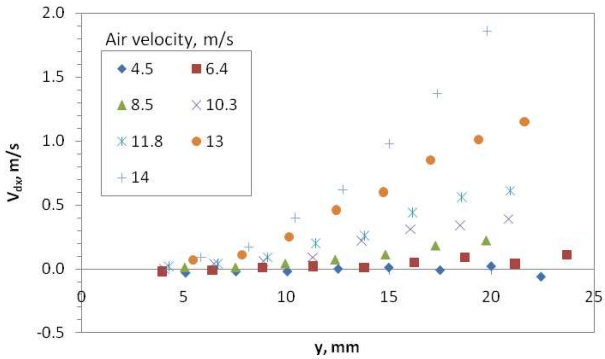

Figure 9. Horizontal velocity component of the droplet

The same analyses were conducted on different droplet sizes and the results showed that increasing droplet Weber number (We_d) leads to delay in the droplet breakup due to the shearing air while increasing droplet Ohnesorge number (Oh_d) boosts the breakup at the same shearing air velocity. In addition, bigger droplets (small Oh_d) are more likely to deform at the same shearing air velocity.

Impact outcomes

As previously mentioned the main aim of this paper is to investigate the interaction of a single droplet with shear-driven films. The analysis of film thickness, surface wave patterns and droplet deformation which are presented in previous sections were essential to identify the characteristics of the impact.

Figure 10 shows two regime maps of the impact outcomes for two droplet sizes of 2.4mm (We_d=183) and 3.8mm (We_d=163). On the map transition regimes for the film surface waves illustrated before in Figure 5 are shown in solid lines. The transition boundaries of the primary droplet deformation and breakup during its movement in the shearing air are also plotted by dotted lines. The 2.4mm droplet (Figure 10- a) has a spherical shape at the moment just before the impact at shearing air velocity up to 12.5m/s and a bag is produced at higher shearing air velocities as it is illustrated in the previous section. The larger droplet (3.8mm, Figure 10- b) shows more deformation types before it breaks up in a multimode breakup [8].

Figure 11 shows sequences of the impact outcomes at different experimental setting. At low air velocities the impact results in crown formation (Figure 11i). In this case no secondary droplets were produced after the impact. At higher air velocities the impact results in secondary droplets where they are produced either from the crown due to droplet momentum (Figure 11ii) or due to the breakup of the crown rim by the shearing air (Figure 11iii). In some cases breakup due to the momentum of the droplet and due to the shearing air happen at the same time. After the impact and the generation of secondary droplets small droplets entrain downstream with the shearing air, while larger droplets fall on the moving film near the impact point and in most cases they coalesce with the moving film.

As shown in Figure 10b increasing the air velocity results in that the droplet breaking up in the air through the well known bag and stamen breakup mechanism [6-8]. In this case the droplet breaks up during or before the impact and different sizes of droplets and ligaments are produced. According to their size they fall somewhere downstream of the breakup point. Figure 11v shows a droplet break up in multimode process (bag and stamen). The lower part of the bag hits the moving film and coalesces with it, which decelerates the movement of the upper part of the bag and lets it break up due the shearing air.

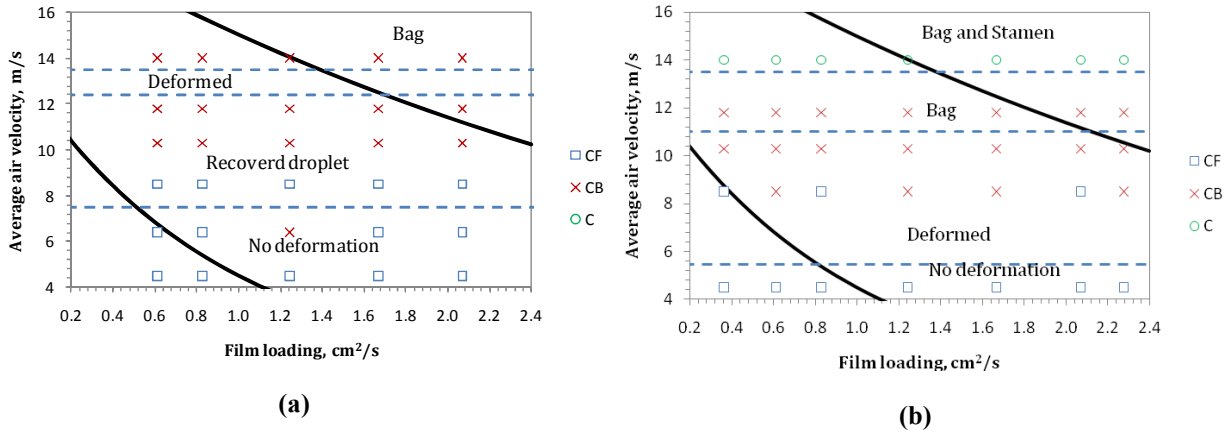

Figure 10. Impact outcomes on L_f-V_g map for 2.4mm droplet (a) and 3.8mm droplet (b). The legend shows impact outcomes ;CF stands for crown formation, CB stands for crown breakup and C stands for coalescence

Taking a general look at the above regime maps (Figure 10), one finds that the shearing air velocity is the parameter that has an important effect on the impact. The surface waves of the moving film seems to have no effect on altering the impact outcomes, however, it might have an important effect on the way that the splash occurs. Comparing Figure 11ii and Figure 11iii shows that the crown might breakup from the upstream or down stream side.

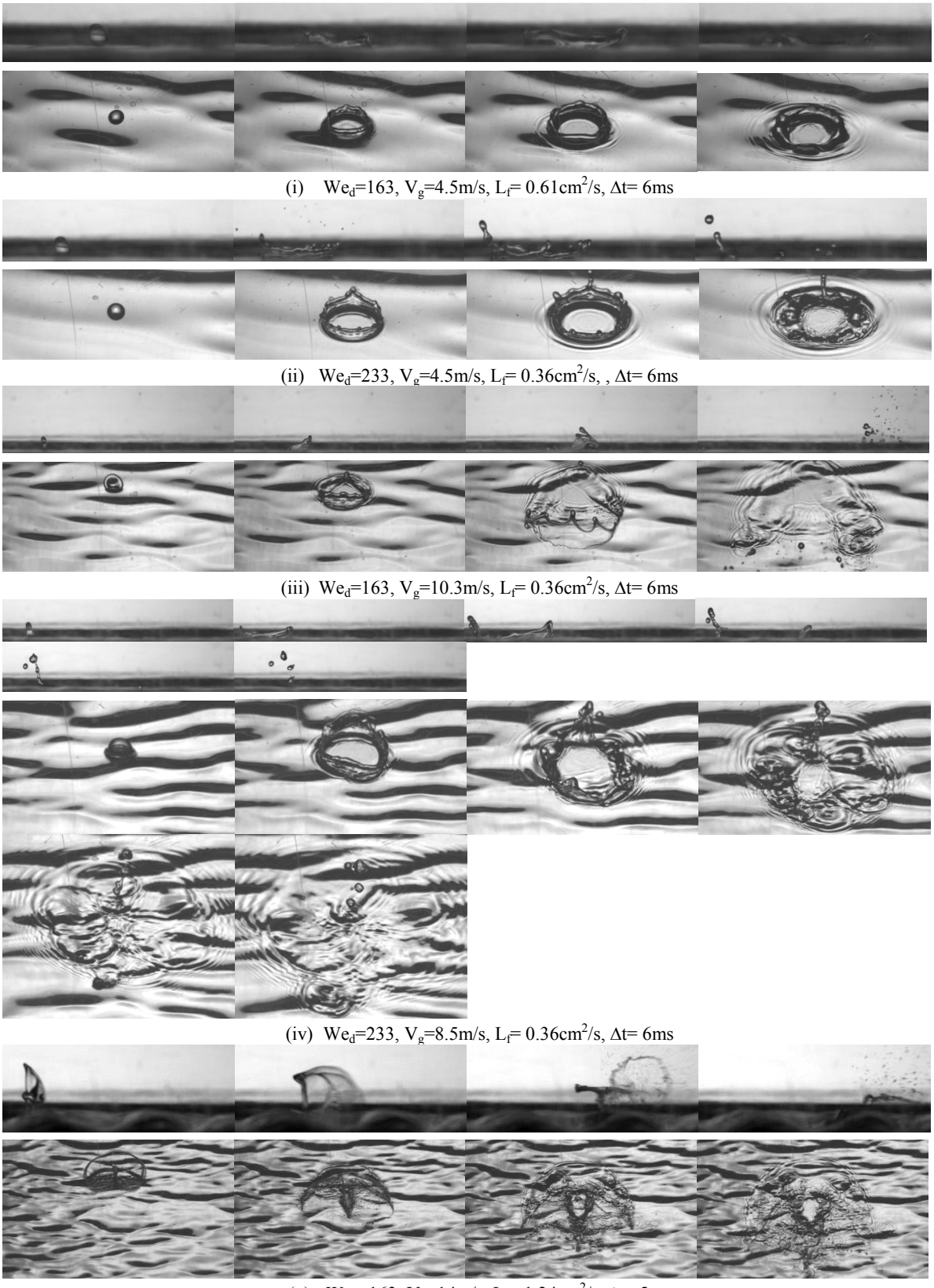

(i) We_d=163, V_g=4.5m/s, L_f= 0.61cm^2/s, Δt= 6ms

(ii) We_d=233, V_g=4.5m/s, L_f= 0.36cm^2/s, , Δt= 6ms

(iii) We_d=163, V_g=10.3m/s, L_f= 0.36cm^2/s, Δt= 6ms

(iv) We_d=233, V_g=8.5m/s, L_f= 0.36cm^2/s, Δt= 6ms

(v) We_d=163, V_g=14m/s, L_f= 1.24cm^2/s, Δt= 2ms

Figure 11. Images of impact outcomes at different experimental setting (i to v). For each case the side images are above the corresponding angled plan images; air and water flow directions are from left to right in the side images and from up to down in the plan images.

Figure 12 shows the impact outcomes for spherical (non-deformed) droplets obtained within all experiments on K-Re_f and K-h_f^* maps, where K is known as a splashing parameter and defined as K=We.Oh$^{-0.4}$. The transition from deposition to splashing should occur at K=2,100 for the impact on static liquids [9, 10].

The figure shows that the transition between splash and deposition occurs around K=2,100. The results suggest that the criterion for the splash/deposition threshold is not influenced by the film movement at law film velocities which agrees with results obtained previously for the impact on slow moving films [4].

Although the maps show either splashing or coalescence at a single impact point, the impact at two adjacent points in some cases presents a noticeably different splash structure which results in a big difference in the size of the produced secondary droplets. This might be a result of the change of the film thickness due to the change in the air or water flow rates or due to the effect of the film surface waves. In order to understand the effects of the surface waves on the splash structure, conducting farther detailed experiments investigation that can visualize the interaction between droplets and surface waves are necessary.

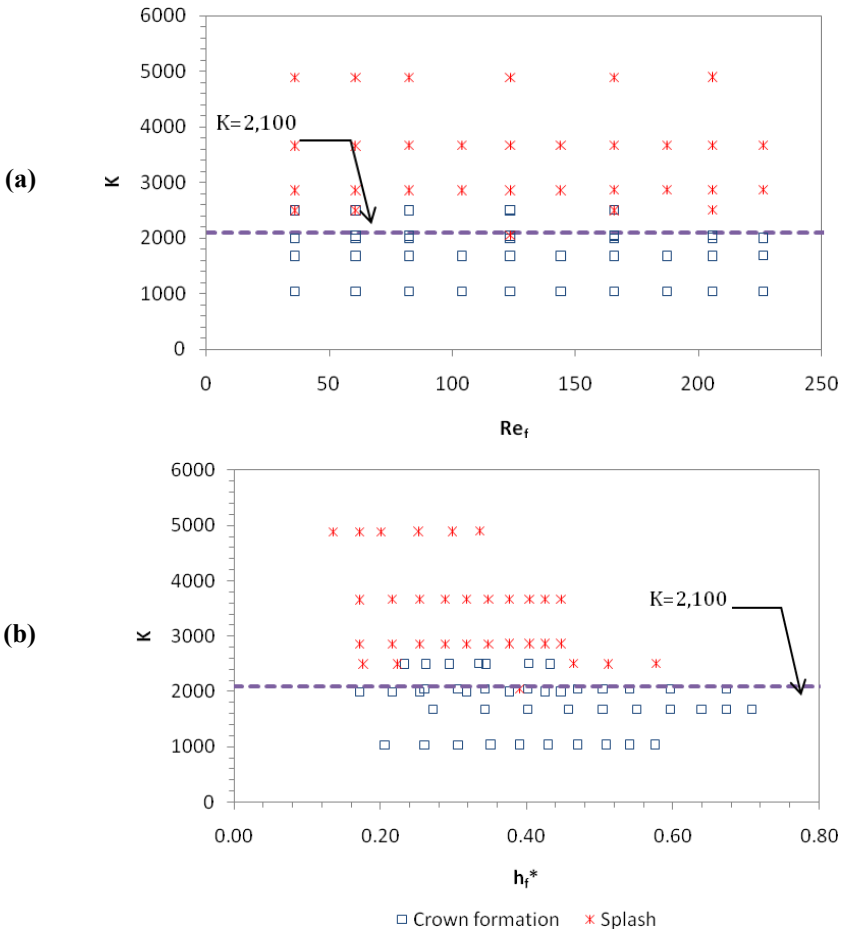

Figure 12. Impact outcomes for spherical droplets plotted on; **a.** *K-Re_f* map **b.** *K- h_f^** map

Conclusions

An experimental investigation of the interaction between a single water droplet and a shear-driven film is presented in this paper. Specific regime maps are presented in this work and they show the effect of different parameters on the impact process such as shearing air velocity, water film flow rate and droplet deformation. Three types of impact are observed within this experiment:

- The impact of spherical droplets which happens when the shearing air velocity is small. The transition between splash and deposition for spherical droplet agrees with the published results obtained for droplet impact on static films and the droplet properties are the most dominant parameter in this case. However, the structure of the impact process is clearly different from the static case.
- The impact of deformed droplets that occur at medium air velocities. The obtained regime maps show that this deformation leads to enhancement of the splashing.

- The impact of highly deformed drops which happens at high air velocities. In this case the droplet takes a shape of bag or bag and stamen with a very thin wall thickness. Due to the weak structure of these highly deformed drops the preferred outcome of the impact is coalescence.

Although the shearing air has an important effect on the interaction process before the impact by deforming the droplet and confining the film thickness, it also influences the impact process during and after the impact by deforming and breaking up the crown rim.

The surface waves on the moving water film are considered to have a negligible effect on defining the impact outcomes. This is due to the fact that the droplets are at least 5 times larger than the surface wave amplitudes of the moving film.

The present work has shown that the phenomenon of droplet impact on shear driven film is of extreme complexity due to the large number of parameters affecting the process. Further experimental and modelling work is necessary in order to reveal the effect of these parameters especially for smaller droplets and high velocity films.

Nomenclature

C	Coalescence
CB	Crown breakup
CF	Crown formation
d	Primary droplet diameter [mm]
h_f	Average film thickness [mm]
h_f^*	Dimensionless film thickness = h_f/d
K	Splash parameter =$WeOh^{-0.4}$
L_f	Film loading [$cm^2.s^{-1}$]
V	Average velocity [$m.s^{-1}$]
We	Weber number
Re	Reynolds number
Oh	Ohnesorge number
y	Vertical distance from top of the duct [mm]
Δt	Time difference between two images

Subscripts

d	Droplet
g	Gas
f	Film
x	Horizontal distance

Acknowledgement

The corresponding author acknowledges Libyan cultural affairs for sponsoring his PhD research. Authors thank the ESPRC who provided the Photron high speed imaging system and finally, we thank Dr Budi Chandra (University of Nottingham) for his help in setting up some measurements.

References

[1] Rein, M, *Fluid Dynamics Researsh* 12:61-93(1993).

[2] Ebner, J., Gerendas, M., Schafer, O., and Wittig,S., *Journal of Engineering for Gas Turbines and Power 124*:874-880 (2002).

[3] Samenfink, W., Elsäßer, A., Dullenkopf, K., and Wittig, S., *International Journal of Heat and Fluid Flow* 20: 462-469 (1999).

[4] Alghoul, S., Eastwick, C., and Hann, D., *Experiments in Fluids*, (submitted November 2009)

[5] Eastwick, C., Huebner, K., Azzopardi, B., Simmons, K.,Young, C., Morrison,R. *Proceedings of GT2005: ASME Turbo Expo 2005: Power for Land, Sea and Air*, Nevada, USA, 2005, pp. 1-6

[6] Azzopardi, B. J., *International Journal of Multiphase Flow* 23:1-52 (1997)

[7] Joseph, D.D., Belanger, J., and Beavers G.S.,, *International Journal of Multiphase Flow*. 25: 1263-1303. (1999)

[8] Guildenbecher, D.R., Lo´pez-Rivera, C. , and Sojka, P.E*., Experiments in Fluids* 46:3 (2009)
[9] Okawa, T., Shiraishi, T. and Mori, T., *Experiments in Fluids,* 44(2): 331-339 (2008)
[10] Okawa, T., Shiraishi, T. and Mori, T., *Experiments in Fluids,* 41(6): 965-974.(2006)